Science of the Total Environment 643 (2018) 793–806

Contents lists available at ScienceDirect

Science of the Total Environment

journal homepage: www.elsevier.com/locate/scitotenv

# Riverine dissolved organic carbon in Rukarara River Watershed, Rwanda

Fabien Rizinjirabake [a,b,*], Abdulhakim M. Abdi [a], David E. Tenenbaum [a], Petter Pilesjö [a]

[a] Department of Physical Geography and Ecosystem Science, Lund University, Sweden
[b] Department of Biology, College of Science and Technology, University of Rwanda, Rwanda

## HIGHLIGHTS

- Eight percent of daily net carbon produced in the watershed is lost through rivers.
- Stream in natural forest had more dissolved organic carbon (DOC) than those in croplands.
- Flow volume and stream DOC had a positive relationship in the watershed.
- Stream DOC concentration and lag time is linked to topography, land use and cover

## GRAPHICAL ABSTRACT

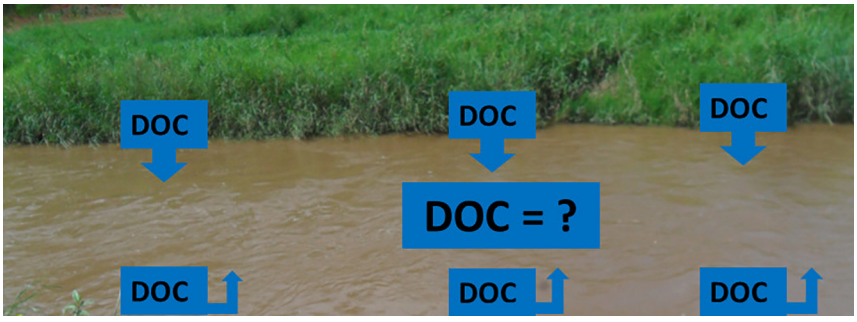


## ARTICLE INFO

*Article history:*
Received 24 October 2017
Received in revised form 11 May 2018
Accepted 15 June 2018
Available online xxxx

Editor: R Ludwig

*Keywords:*
Dissolved organic carbon
Watershed
Land use and land cover
Stream water
Rwanda

## ABSTRACT

Dissolved organic carbon (DOC) loading is rarely estimated in tropical watersheds. This study quantifies DOC loading in the Rukarara River Watershed (RRW), a Rwandan tropical forest and agricultural watershed, and evaluates its relationship with hydrological factors, land use and land cover (LULC), and topography to better understand the impact of stream DOC export on watershed carbon budgets. The annual average load for the study period was 977.80 kg C, which represents approximately 8.44% of the net primary productivity of the watershed. The mean daily exports were 0.37, 0.14, 0.075 and 0.32 kg C/m$^2$ in streams located in natural forest, tea plantation, small farming areas, and at the outlet of the river, respectively. LULC is a factor that influences DOC loading. The quick flow was the main source of stream DOC at all study sites. Stream DOC increases with increasing water flow, indicating a positive relationship. Thus, the expectation is that a change in land cover and/or rainfall will result in a change of stream DOC dynamics within the watershed. Topography was also found to influence the dynamics of stream DOC through its effect on overland flow in terms of drainage area and total length of flow paths. Tea plantations were located in areas of high drainage density and projected increase of rainfall in the region, as a consequence of climate change, could increase stream DOC content and affect stream water quality, biodiversity, balance between autotrophy and heterotrophy, and bioavailability of toxic compounds within the RRW.



## 1. Introduction

The role of inland waters in the global carbon cycle is now widely recognized at the catchment, regional and global scales (Cole et al., 2007; Battin et al., 2009). Streams receive carbon from in-stream and terrestrial production that is processed or exported downstream (Mattsson et al., 2009; Williams et al., 2010; Alvarez-Cobelas et al.,

* Corresponding author at: Department of Physical Geography and Ecosystem Science, Lund University, Sölvegatan 12, 223 62 Lund, Sweden.
*E-mail address:* fabien.rizinjirabake@nateko.lu.se (F. Rizinjirabake).

https://doi.org/10.1016/j.scitotenv.2018.06.194
0048-9697/

2012). Another source of carbon in rivers is sediment and rock weathering processes in carbonates and gypsum-rich deposits (Salimon et al., 2013). Carbon enters streams mainly through surface runoff and by groundwater as particulate organic carbon (POC), dissolved organic carbon (DOC), and dissolved inorganic carbon (DIC) (Johnson et al., 2006; Aufdenkampe et al., 2011).

This study focuses on DOC since it is the major organic pool in most aquatic ecosystems (Wetzel, 2001). Stream-water DOC is of particular interest because it serves as an important resource for downstream ecosystems (Amon and Meon, 2004; Post et al., 2009; Pagano et al., 2014) and is beneficial for aquatic biota (Sucker and Krause, 2010). Organic carbon in streams serves as an important modulator because it modifies the influences and consequences of other chemicals and processes (Prairie, 2008). However, changes in DOC levels in water are also of environmental concern: high DOC concentration can affect surface water quality, water metabolism, balance between autotrophy and heterotrophy, nutrient uptake and bioavailability of toxic compounds, and the growth of microorganisms (Munson and Gherini, 1993; Delpla et al., 2009; Fernández-Pérez et al., 2005; Erlandsson et al., 2011; Stanley et al., 2012).

DOC concentration in natural waters has changed over the past few decades; for example, in some areas in North America and northern Europe, it may have doubled (Evans et al., 2005; Monteith et al., 2014; SanClements et al., 2012; Pagano et al., 2014). In a few other areas, a decrease or no increase of DOC in waters was reported (Pagano et al., 2014). Regarding the increase of DOC in natural waters, its drivers in some areas are up for debate. Possible factors include changes in air temperature (Freeman et al., 2001), increased precipitation (Worrall and Burt, 2008; Sucker and Krause, 2010), land use changes (Findlay et al., 2001; Sucker and Krause, 2010), increased atmospheric carbon dioxide (Harrison et al., 2008; Sucker and Krause, 2010; Kane et al., 2014) and decreased atmospheric sulfur deposition (Fowler et al., 2005; Sucker and Krause, 2010; Rowe et al., 2014) and atmospheric nitrogen deposition (Singh et al., 2016). Pagano et al. (2014) mention the combined effect of increased atmospheric $CO_2$ concentration and temperature. This increased atmospheric $CO_2$ stimulates plant primary production (Freeman et al., 2004) whereas global warming may influence DOC export by altering decomposition and mineralization of organic matter (Worrall et al., 2003), water budget and discharge, which then increases DOC concentrations (Hongve et al., 2004). Consequently, an increase of DOC in freshwaters may be linked with climate change, it is therefore important to monitor temporal variations of DOC concentration in natural waters to anticipate climate impacts on carbon dynamics and water resources.

Most studies of DOC changes in waters have been performed in temperate ecosystems in North America and Europe. Thus, there is a need to monitor DOC changes in waters in other geographical areas, such as tropical regions, where precipitation and temperature are projected to continue to increase (Paeth et al., 2009). For example, in Rwanda, temperatures have increased 1.4 °C from 1970 to 2008, and this increase is projected to reach 1.5 °C to 3 °C by the 2050s (Hove et al., 2010). Average annual rainfall increased about 10% during the same time interval (Warnest et al., 2012). It follows that changes in climate will alter water budgets in tropical watersheds, with implications for DOC in natural waters. It is important to monitor how hydrological variability can affect DOC in natural waters in tropical watersheds in order to better understand this issue and its implications for the global carbon budget.

Studies suggest that tropical rivers exhibit the highest riverine DOC flux to oceans (Gu et al., 2009; Bouillon et al., 2014), but their inclusion in carbon budgets stems from datasets that are missing well-defined values in the tropics since most studies of riverine DOC have been performed in temperate and arctic rivers (Stedmon et al., 2011; Spencer et al., 2012; Lambert et al., 2015). Recent research (e.g. Palviainen et al., 2016; Ren et al., 2016; Singh et al., 2016) has shown that land cover is a useful predictor of riverine DOC in temperate biomes, but the situation may be different in tropical regions.

The objective of this study is to determine the relationship between stream water DOC loading, hydrological factors, topography and land cover in a tropical watershed for a better understanding of the impact of stream DOC export on watershed carbon budget. This study specifically characterizes the spatial and temporal variation of stream DOC and describes the relationship between stream DOC, water level, water discharge and land cover. It estimates the DOC loading in the Rukarara River and some of its tributaries, and the loss of DOC through fluvial export compared to the net primary productivity of the watershed. We hypothesize that the variability in hydrology and land cover will alter runoff, discharge characteristics and carbon dynamics in tropical watersheds, and this will be expressed in variable export of soil DOC into streams.

## 2. Material and methods

### 2.1. Study area

The study was carried out in the Rukarara River Watershed (RRW), a catchment that drains an area of 493.5 $km^2$ (Fig. 1a) in southwestern Rwanda. The catchment landscape is composed of mountainous terrain with elevations from 1541 to 2924 m., and slopes from 0° to 68°. Annual precipitation ranges from 1300 to 1450 mm, and the temperature from 15 °C to 25 °C. The soils are acid ($3.6 < pH < 5.0$) and mainly of the Ultisol, Entisol, and Inceptisol types. Across the watershed, 13 main streams drain waters into Rukarara River.

The watershed is a part of the Nyungwe Natural Forest, and also includes cultivated forests and croplands with annual or perennial crops. Annual crops include, for example, common beans, maize, and banana plantations; the perennials are primarily tea and cassava. All crops, except tea, are food crops used by small farmers who use simple handheld tools like hoes to prepare their cropland. The farmers rotate groups of crops, for example, common bean and sorghum, and also mix in others like maize. Industrial fertilizers are normally used for tea plantations. Most farmers use organic manure for other crops. As is the case for most Rwandans, the primary source of energy for inhabitants in Rukarara River Watershed is mostly biomass in form of wood, branches, leaves and crop residues.

### 2.2. Data collection and analysis

#### 2.2.1. Water stage data

To collect data of stream stage, gauging stations were installed at the four sites (Fig. 2). At each site, an automatic pressure transducer was installed for recording the water level, as a function of pressure, every 15 min. The transducers were protected by iron stilling wells, fixed with concrete and closed with padlocks. Water stage data were collected from March 2015 to February 2017 at four sites namely natural forest, tea, farm and outlet (Fig. 2). Water stage data were used together with flow data to produce rating curves. The rating curves were used to predict non-measured flow data that have been used in estimation of annual DOC load.

#### 2.2.2. Water velocity and flow data

On several occasions, data of velocity were measured using small and middle size current meters by the Six-Tenths-Depth method (Dingman, 1984). A medium size current meter (current meter number: C31 261020 and propeller number: 2-252132) was used for velocity measurement at the outlet, and the tea and natural forest streams. A current meter appropriate for the smallest flows (current meter number: C2 253194 and propeller number: 272477) used for measuring velocity data for the farm stream. The stream flow was measured along a number of vertical segments lying along the cross sectional width of the channel. The number of verticals depended on the width of the stream and was determined in the sense that the flow in each subsection should be <5% of the total and the difference in velocity values

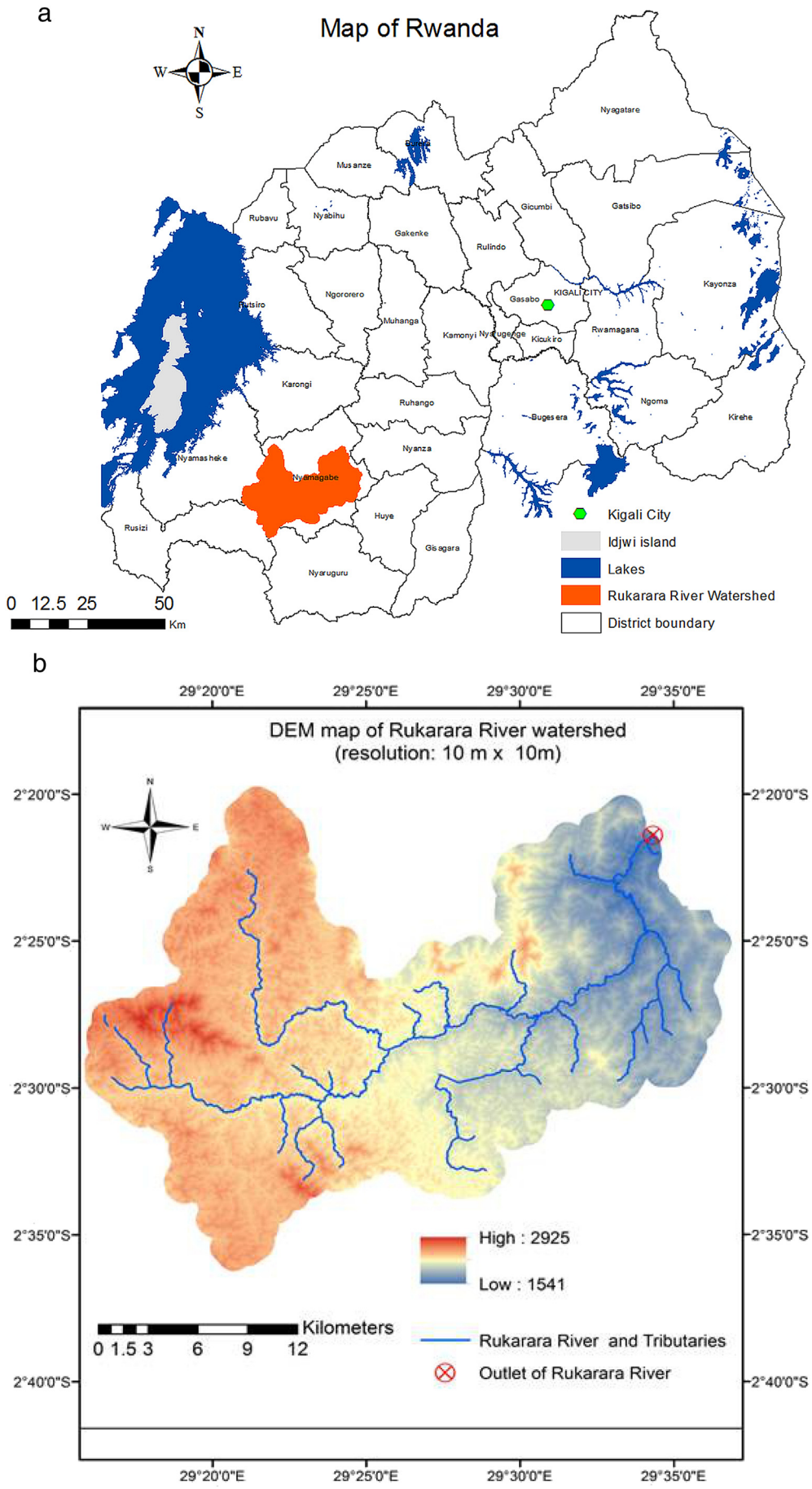


**Fig. 1.** a. Location of the study area in the Nyamagabe District in the south west part of Rwanda. b. DEM map of the study area.

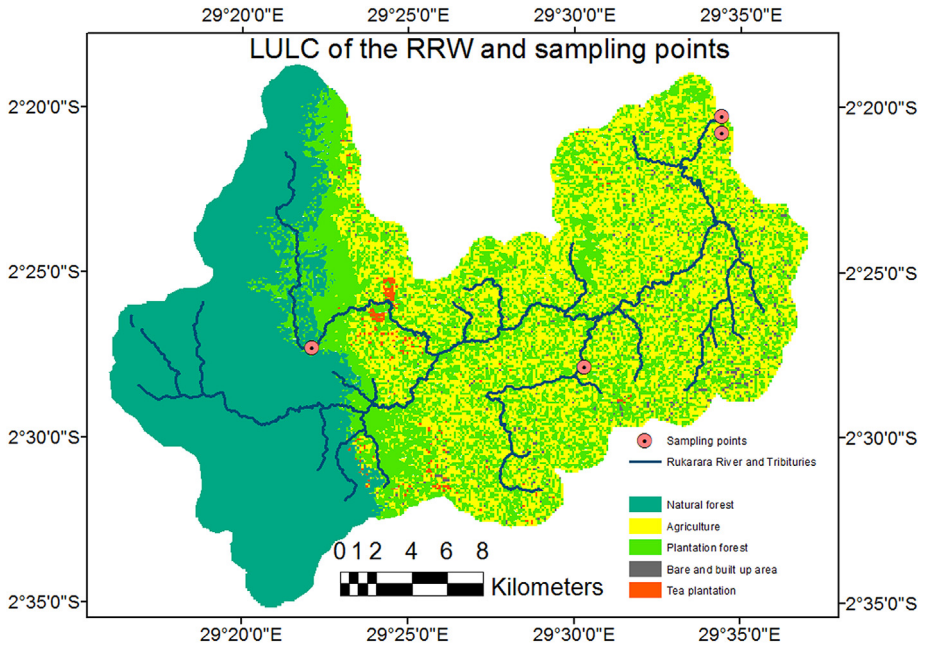


**Fig. 2.** Location of sampling points of water level, water flow and stream DOC in the study area.

between two adjacent points should not be >20% of the higher value (Baldassarre and Montanari, 2009). The number of verticals was 22, 15, 13 and 9 at respectively outlet, natural forest, tea and small farm sites. The distance between two successive verticals was 50 cm for Rukarara River, 40 cm for tea and natural forest streams and 10 cm for the farm stream.

Velocity (V) was calculated using the following Eqs. (1) and (2) for the small size current meter and Eqs. (3) and (4) for the medium size current meter:

$$n<2.58, V = 0.0634n + 0.012 \quad (1)$$

$$n>2.58, V = 0.0572n + 0.028 \quad (2)$$

$$n<0.35, V = 0.4774n + 0.015 \quad (3)$$

$$n>0.35, V = 0.5086n + 0.015 \quad (4)$$

where $n$ is the number of propeller revolutions per second.

*2.2.3. Water flow data*

Instantaneous stream flow ($Q_i$) ($m^3/s$) data were estimated by multiplying the velocity (m/s) of a section and its area ($m^2$) determined by the mid-section method (Dingman, 2008) using the rectangular formula. The total stream flow was estimated by summation of all section flows. These measured flow data were used to describe the relationships between flow, stream water stage, and DOC and to analyze contribution of quick flow and groundwater to the total stream flows.

*2.2.3.1. Analysis method for relationship between stream water stage and flow.* The relationships between stage and flow or rating curves were produced using contemporaneous measures of water stage and stream flows. The power-law function (Eq. (5)) was also used for rating curves.

$$Q_i = aH_i^b \quad (5)$$

where $Q_i$ is the instantaneous flow ($m^3/s$), and $H_i$ is the water stage.

The rating curves were evaluated and used to estimate flow from stage data. The rating curves were evaluated using the Nash-Sutcliffe efficiency (NSE) (Nash and Sutcliffe, 1970), a normalized statistic that determines the relative magnitude of the residual variance compared to the data variance (Moriasi et al., 2007). NSE is commonly used, as it provides extensive information on reported values and was recommended by Legates and McCabe (1999).

NSE ranges between negative infinity and 1 where NSE values between 0 and 1 indicate that model predictions are better than simply using the mean of measurements. NSE is computed as follows:

$$NSE = 1 - \frac{\sum_{i-1}^{i}(Obs_i - Mod_i)^2}{\sum_{i-1}^{i}\left(Obs_i - \overline{Obs_i}\right)^2} \quad (6)$$

where $Mod_i$ and $Obs_i$ are the model-predicted and measurement-based flow for a sub-watershed and $\overline{Obs_i}$ stands for observed mean flow.

*2.2.3.2. Analysis method for the relationship between stream water DOC and flow.* The relationship between stream water DOC and flow is known to characterize the variation of the solute concentration in response to water flow variability (Laraque et al., 2013). The relationship has also important implications in predicting stream DOC fluxes with consideration to landscape environmental conditions (Jawitz and Mitchell, 2011). For this paper, the relationship between stream DOC and flow was functionally described using the power function:

$$DOC = aQ_i^b \quad (7)$$

where DOC is the instantaneous concentration of stream DOC (mg C/L), $Q_i$ is the discharge ($m^3/s$) corresponding to the sampling date and $a$ and $b$ are the regression coefficients. The coefficient $b$ was used as an index to characterize the response of stream DOC to changes in water flow according the Moquet et al. (2016) method. According the method, if the $b$ is zero, the solute concentration variability is low and independent of water flow. If the $b$ is <0, the solute concentration decreases with increasing water flow. The solute concentration increases with increasing flow if $b$ is >0. A large value of $b$ corresponds to low sensitivity of the solute concentration (Moquet et al., 2016).

*2.2.3.3. Stream flow separation.* The aggregate of the different sources that contribute to water arriving at the stream channel represents total stream flow. This total stream flow can be subdivided into quick flow and baseflow components. The quick flow component is the direct

response to a rainfall event including overland flow or runoff, interflow and direct precipitation. The baseflow component is the flow derived from the slow, gradual delivery of groundwater and soil water to the channel. In this paper, to separate the total stream flow into its components, we used the statistical method known as flow-duration-curve (FDC). A flow duration curve displays the percentage of time that a given flow is equalled or exceeded for a particular catchment (Li et al., 2010; Welderufael and Woyessa, 2009; Brodie and Hostetler, 2005; Lyne and Hollick, 1979). The FDC method is constructed for the entire record of flow measurement or for specific time periods (days, months, seasons, etc.). In this paper, daily flow data were used. The percentage of the probability (P) a given flow is equalled or exceeded is calculated as follows:

$$P = 100 * \frac{m}{n+1} \tag{8}$$

where $m$ is the rank number when the flows are arranged in decreasing order; and $n$ is the total number of observations.

The flow-probability relationship is typically presented as a log-normal plot and provides information on the baseflow component of stream flow. According Brodie and Hostetler (2005), the median flow (Q50) is the flow that is equaled or exceeded 50% of the time. The part of the curve with flows below the median flow represents low-flow conditions. The baseflow is significant (and the quick flow insignificant) if the low-flow part of the curve has a low slope and vice versa. The contribution of the groundwater was estimated by the ratio between Q90 and Q50.

*2.2.4. Stream DOC concentration*

Stream DOC concentrations (mg C/L) were analyzed from stream water samples collected during the period from March 2015 to March 2017 at four sites located in natural forest, tea plantation, farm and, outlet sub-catchments. The sampling sites were selected at straight river reaches with a channel bank that is relatively uniform. The samples were collected at a biweekly frequency in polyethylene bottles of 25 mL and transported for analysis to the chemistry laboratory of the College of Science of the University of Rwanda, Huye Campus. Bottles were not totally filled in order to allow the addition of 1 mL of sulfuric acid ($H_2SO_4$) to reduce the microbial activity before laboratory analysis. In the laboratory, water samples were first filtered using nylon membrane filters of a pore size of 0.80 μm to remove large particles, and then nylon membrane filters of pore size of 0.45 μm were used to remove particulate organic carbon. Analysis of stream water DOC concentration was performed using a TOC analyzer (the Sievers InnovOx Laboratory TOC Analyzer). The analyzer oxidizes organic compounds to $CO_2$ at high temperatures in a sealed reactor using an oxidizing agent. The concentration of DOC in filtered water samples is the difference between the total carbon and the inorganic carbon concentrations. Stream DOC concentration means (mg C/L) were estimated for each sampling site using biweekly stream water DOC data, and compared using *t*-tests.

*2.2.5. DOC loading*

Annual DOC loads were estimated using the flow-weighted (FW) method that calculates the load by multiplying the flow-weighted mean concentration by the total flow (Littlewood et al., 1998; Huang et al., 2012; Elwan et al., 2015). The FW method was recommended alongside the flow stratified (FS) method for estimating annual river loads because it takes into account hydrological response (Elwan et al., 2015). The following equation was selected because it is among the best performing method with minimized uncertainty (Cassidy and Jordan, 2011).

$$L = mQ_T \frac{\sum_{i=1}^{n} C_i Q_i}{\sum_{i=1}^{n} Q_i} \tag{9}$$

where $L$ is the annual estimated load (kg DOC); $m$ is the unit conversion factor, $Q_T$ is the total annual flow ($m^3$); $C_i$ and $Qi$ are concentration (mg C/L) and average daily flow measured at the $i$th day ($m^3$/s), and $n$ is the number of measurements loading type. Daily and annual loadings were calculated for all sites whereas annual DOC yield (load per unit area) was calculated only at the outlet of the RRW. The annual DOC loading was used to evaluate the impact of stream DOC loading on carbon sequestration within the RRW.

*2.2.6. Time of concentration and the lag time*

The time of concentration ($T_c$) and the lag time ($T_{lag}$) were estimated to better understand the impact of land use and land cover (LULC) on DOC loading, for example during rain events. The $T_c$ defines the time required for the overland flow from different LULC classes to exit the RRW. $T_c$ is the time required for runoff to travel from the hydraulically most distant point to the outlet of a watershed (Garg and Garg, 2001). The total time of concentration is obtained by adding the overland flow ($T_{ov}$) and the channel flow ($T_{ch}$) time of concentration. $T_{ov}$ represents the necessary time that runoff to reach a water channel whereas $T_{ch}$ is the time it takes to that the runoff to reach the outlet point (Roussel et al., 2005). The $T_{lag}$ is the time difference between the center of the rainfall event and the runoff peak (DHI, 2011). The flow path length values were calculated in ArcMap 10.2.2 using a 10 m Digital Elevation Model (DEM) (Fig. 1b) provided by the Centre of Geographical Information System and Remote Sensing of the University of Rwanda.

The $T_c$ and the $T_{lag}$ were calculated for fore LULC classes: natural forest (NF), plantation forest (PF), agriculture (farm plus tea plantations) (AGL) and bare and built up areas (BBA). $T_c$ and $T_{lag}$ were calculated using respectively the Kerby-Kirpich method (Roussel et al., 2005) and the Soil Conservation Service method used by Costache (2014). The $T_c$ calculated by the Kerby-Kirpich method is the summation of the overland flow time of concentration ($T_{ov}$) calculated according Wanielista et al. (1997) method (Eq. (10)) and the channel-flow component of runoff ($T_{ch}$).

$$T_{ov} = K(LNS^{-}0.5)^{0.467} \tag{10}$$

$$T_{ch} = K\,L^{0.770}\,S^{-0.385} \tag{11}$$

$$T_{lag} = T_c * 0.6 \tag{12}$$

where $T_c$ is the time of concentration in minutes, $K$ is a units conversion coefficient (K = 0.83 for SI units), $L$ is the flow path length in meters, $N$ is a dimensionless Kerby retardance roughness coefficient and $S$ is the dimensionless overland or main channel slope of the terrain of the interest. The main channel slope is calculated by dividing the change in elevation from watershed divide by the curvilinear distance of the main channel between the watershed divide and the outlet (Roussel et al., 2005). LULC altitude data required for calculation of overland and channel slopes, were extracted from a 10 m DEM (Fig. 1b) of the study watershed based on the classified land cover image obtained in Jun 2015 from RapidEye. The Kerby retardance coefficients ($N$) were from Chin et al. (2000) and were used after an approximate equivalence was taken into account: The following $N$ values were used: 0.30 for farm and built up areas, 0.40 for tea plantations, 0.60 for tree plantations and 0.80 natural forest. The flow length data were generated from a flow direction raster that was first generated from a pit-filled version of the 10 m DEM (Fig. 1b) of the RRW using the Hydrology toolbox available in ArcGIS 10.2.2 Spatial Analyst.

*2.2.7. Net primary productivity*

Moderate Resolution Imaging Spectroradiometer (MODIS) net primary productivity (NPP) data of the whole RRW for the period from 2000 to 2014 were used to estimate the level carbon production and loss (%) due to stream DOC loading in the study watershed. NPP data (MOD17A3: 1000 m × 1000 m) were produced by the NASA Earth

Observation System (EOS) program and obtained from LP DAAC website (https://modis.ornl.gov/cgi-bin/MODIS/global/subset.pl). The data were produced using the MOD17 algorithm based on the light use efficiency method (Monteith, 1972).

The NPP data were obtained as geoTIFF files which were analyzed in ArcMap 10.2.2 and used to calculate daily NPP of the study area. The daily NPP was compared to daily DOC exportation to estimate the importance of stream DOC loading on the carbon sequestration within the study watershed.

*2.2.8. Land use and land cover*

The LULC classes were determined based on a 6.5 m ground resolution RapidEye satellite image of the study area. We used a feedforward artificial neural network (ANN) in the ENVI 5.2 software package to classify the satellite image into the predetermined land cover classes. ANN is a non-parametric machine learning technique based on a model of interconnected artificial neurons (nodes) distributed across three or more layers and designed to mimic biological neural networks (Qiu and Jensen, 2004). The feedforward aspect of the ANN means that the signals can only travel in one direction. In a multilayer ANN, each processing step computes values based on a weighted sum of its inputs. The new values are then fed as inputs into the next layer, and this process repeats through all the layers up to the output. The basic structure of ANN comprises three layers, their nodes and weighted links. The nodes in the input layer receive data and pass it to the hidden layer. The hidden layer is where transformations are applied to the inputs using an activation function. The activation function provides the gradient for calculating error signal back-propagation for supervised learning (Kavzoglu and Mather, 2003), and is designed to minimize the mean square error between the reference data and the output. As the network undergoes training iterations, the nodes that have the lowest mean square error are weighted more heavily (Berberoglu and Curran, 2004).

We used a logistic sigmoid activation function in the ANN classifier and applied the following settings: training threshold contribution = 0.9, training rate = 0.2, training momentum = 0.9, training RMS exit criteria = 0.1, number of training iterations = 1000, number of hidden layers = 1. The accuracy of the classification was assessed using Cohen's Kappa coefficient (Cohen, 1960), user/producer accuracy and omission/commission error. The Kappa coefficient is a statistic that measures the agreement between reference data and ANN classifier. The Kappa coefficient has a range between 0 and 1, where 0 is no agreement and 1 is perfect agreement. Producer's accuracy indicates the proportion of correctly classified pixels relative to all the pixels of that class in the reference data. User's accuracy indicates the proportion of correctly classified pixels relative to all the pixels classified as that class by the ANN classifier. The omission error indicates underestimation, i.e. classification of a pixel that belongs to a certain class into other classes, and is calculated by subtracting the producer's accuracy (in %) from 100. The commission error indicates overestimation, i.e. incorrect classification of a pixel that belongs to another class into the class in question, and is calculated by subtracting the user's accuracy (in %) from 100 (Janssen and Van der Wel, 1994). An omission error in one class is counted as a commission error in another class. ENVI also calculates the overall accuracy of the classification by dividing the sum of correctly classified pixels by the total number of pixels. However, unlike the Kappa coefficient, overall accuracy does not account for omission and commission errors in the classified data (Congalton and Green, 2008). We calculated also individual Kappa coefficient values for each class using the Rossiter method (Rossiter, 2004) to determine which LULC classes are well classified. The individual Kappa values are restricted to one row ($\overline{K_r}$) (Eq. (13)) or column ($\overline{K_c}$) (Eq. (14)):

$$\overline{K_r} = \frac{C_i - p_{+1}}{1 - p_{+1}} \tag{13}$$

$$\overline{K_c} = \frac{o_j - p_{j+}}{1 - p_{j+}} \tag{14}$$

where $C_i$ stands for the user's accuracy for the mapped class $i$; $p_{+1}$ for the proportion of mapped data in class $i$, $o_j$ for the producer's reliability of the reference class $j$; and $p_{j+}$ for the proportion of reference data in class $j$.

A spatial distribution index (Eq. (15)) was used to describe the influence of LULC on DOC loading in the Rukarara River. This spatial index (SI) is a number that describes the distribution of a LULC class within a specified area with respect to flow accumulation. The SI equation was defined by Fedorko (2012) as follows:

$$SI = \frac{\sum_{n=1}^{N} W_n S_n P_n}{\sum_{n=1}^{N} W_n S_n \overline{P}} \tag{15}$$

and

$$\overline{P} = \frac{\sum_{n=1}^{N} W_n P_n}{\sum_{n=1}^{N} W_n} \tag{16}$$

where $n$ is the index for each pixel in the watershed; $N$ is the number of pixels in the watershed; $W_n$ is the weight (between 0 and 1) estimated as Kerby retardance roughness for each LULC class; $S_n$ is the flow accumulation value for pixel $n$; and $P_n$ is the proportion of a given LULC class in the pixel $n$. $\overline{P}$ is the proportion of the LULC class in the watershed. LULC weights here were Kerby's retardance coefficients, whereas flow accumulation data were estimated from a flow direction raster that was first generated from a filled version of the 10 m DEM as described above.

*2.2.9. Digital terrain data*

Topography metrics such as slope position and Topographic Wetness Index (TWI) (Beven and Kirkby, 1979), also known as Compound Topographic Index (CTI) (Moore et al., 1991), were calculated to describe the topography of different LULC classes within the RRW to quantify overland flow and therefore the combined effects of LULC and topography on DOC loading. The slope position represents the relative position between the valley floor and the ridge top. It was computed using the method by Deumlich et al. (2010) based on Topographic Position Index (TPI) and slope. According to this method, the slope position varies from 1 to 6; where 1 stands for summit top or ridge, 2 for upper slope, 3 for mid-slope, 4 for flat slope, 5 for lower slope (foot slope, toe slope), and 6 for depression or valley. The TWI is a steady state wetness index and therefore an indicator of potential saturated and unsaturated areas within a watershed. High TWI values areas represent depressions or saturated areas whereas low TWI values areas represent steep slopes or unsaturated areas. Both slope position and TWI values were estimated using the Geomorphometry and Gradient Metrics toolbox (Evans et al., 2014), which was downloaded and installed in ArcGIS. TWI was estimated as follows:

$$TWI = \ln(As/\tan\beta) \tag{17}$$

where $As$ is the area value calculated as (flow accumulation + 1) * (pixel area in $m^2$) and $\beta$ is the slope expressed in radians.

The slope position and TWI values for each LULC class were extracted and summarized in ArcMap 10.2.2. Area percentages of high slope positions (1–4) and low slope positions (5–6) were calculated based on areas (%) of individual slope positions in all LULC classes. Similarly, percentages of high TWI (TWI > mean TWI) and low TWI (TWI < mean TWI) areas were calculated. The LULC classes were compared on the basis of the ratio (%) between areas of high and low TWI values.

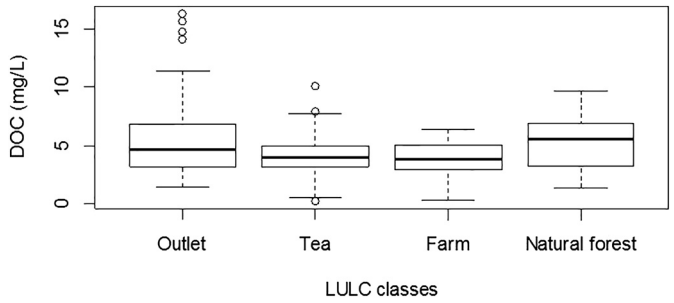


**Fig. 3.** Box plot of DOC concentration in inland waters in the RRW. At the outlet station, DOC is higher than in the tea and farm streams but not than that of the natural forest site. DOC is also statistically different between natural forest, tea and farm streams at the 95% confidence level. There is no statistical difference between DOC observed at the tea and farm sites.

## 3. Results

### 3.1. Stream DOC variation between sites

The results indicate higher concentration of DOC in the natural forest stream compared to the tea plantation and farm streams. The measured DOC means (mg C/L) were 4.98 ± 2.15, 4.06 ± 2.06 and 3.66 ± 1.62 in natural forest, tea, and farm streams, respectively. The DOC concentration at the outlet of the Rukarara River was 5.73 ± 3.75 mg C/L, higher than at all sampled headwater streams (Fig. 3). A two-tailed *t*-test showed a statistically significant difference between streams in the natural forest, tea and farm DOC concentrations at the 95% confidence level. The difference was not, however, significant between the natural forest stream and the outlet, and between tea and farm streams. Regarding the variation of stream DOC, the analysis of coefficients of variation revealed temporal variation. The coefficients of variation were 0.62, 0.49, and 0.46 for the natural forest, tea and farms sites, respectively. The outlet site showed the lowest coefficient of variation of 0.27.

### 3.2. Relationship between stage and flow

Relationships between water stage and flow were performed using 12, 16, 18, and 13 water flow measurements taken in streams at the natural forest, tea plantation and small farming sites, and at the outlet site, respectively. Fig. 4 presents the obtained relationships and their corresponding coefficients of determination ($R^2$). An evaluation of these rating curves showed NSE (Nash-Sutcliffe efficiency) values from 0.83 to 0.88. NSE values are 0.83, 0.88, 0.82, and 0.87, respectively, for natural forest, tea, and farm streams and outlet sites. These NSE values indicate that flow data that were modeled using these rating curve equations are better representations of the measured flows.

### 3.3. Flow component contribution

The flow duration curve analysis revealed that the baseflow component is a very small stream flow component within the RRW. Low flow parts of curves were sloppy in appearance, indicating that discharge to stream under these conditions is not continuous (Fig. 5, A–D). Probability-flow $R^2$ values varied from 0.79 to 0.96 with the lowest coefficient in the steam located in the natural forest. Slopes for the low-flows were steep suggesting small flow contributions from groundwater. The groundwater contributions were, by decreasing order, 2.73%, 1.88%, 1.30%, and 1.20% for the streams in farming area, tea plantations, natural forest, and the large river, respectively. Based on the above analysis results on baseflow and groundwater contributions to stream flow in the RRW, it is clear that the quick flow contributed from rainfall and overland flow is the most important flow. The quick flow may affect the dynamics of stream DOC in the study watershed.

### 3.4. Relationship between stream water DOC and flow

The analysis indicated a weak, but significant, positive relationship between water DOC and flow in the RRW (Fig. 6). The relationship varies between sites and $R^2$ values range from 0.19 to 0.36. The tea site shows the highest $R^2$ and is therefore more linked with water flow compared to other sites. Fitted power functions produce different

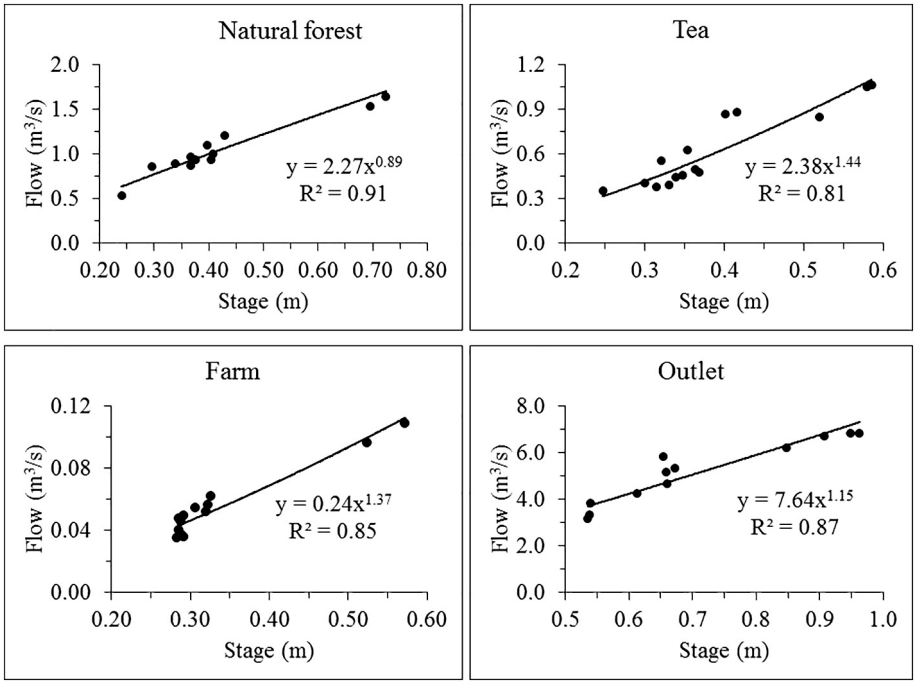


**Fig. 4.** Relationship between stage and flow at the streams and outlet as described by power functions and coefficients of determination ($R^2$) in the RRW.

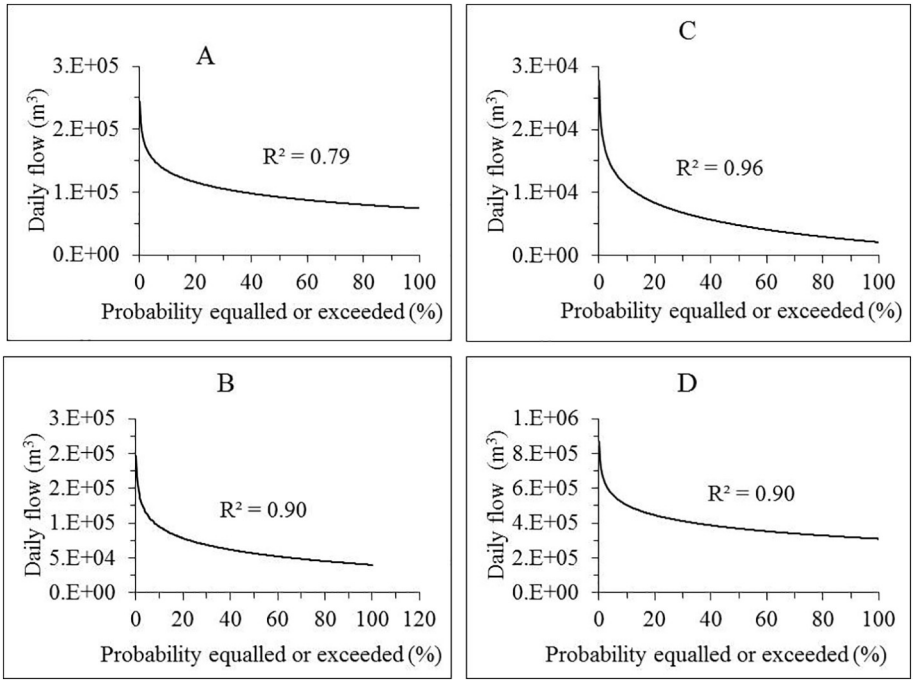


**Fig. 5.** Probability - flow relationships within the RRW for a two-year period from March 2015 to February 2017. Letters A, B, C and D represent the relationship for the stream in natural forest, tea, farm and outlet.

optimal *b* coefficients: 0.38, 0.21, 1.40 and 0.63 respectively for the natural forest, tea, farm and outlet sites. All coefficients are greater than zero indicating that stream DOC concentration increases with increasing water flow at all sites. The farm site shows the highest slope, followed by the outlet site. This means that the stream DOC at this site is less sensitive to stream flow. On the contrary, the natural forest site has the smallest slope coefficient and therefore is the most sensitive to stream flow volume. The *b* values of the relationship between stream DOC and water flow varies from site to site, but they are between 0.21 and 1.40 in the RRW. This result indicates that stream DOC concentrations respond to changes in stream flow volume.

### 3.5. Loads of DOC in the RRW

Relationships described between stage and flow data were revealed to be "very good" according to the Moriasi et al. (2007) ranking, and therefore used in estimating annual flow and DOC loading at the outlet

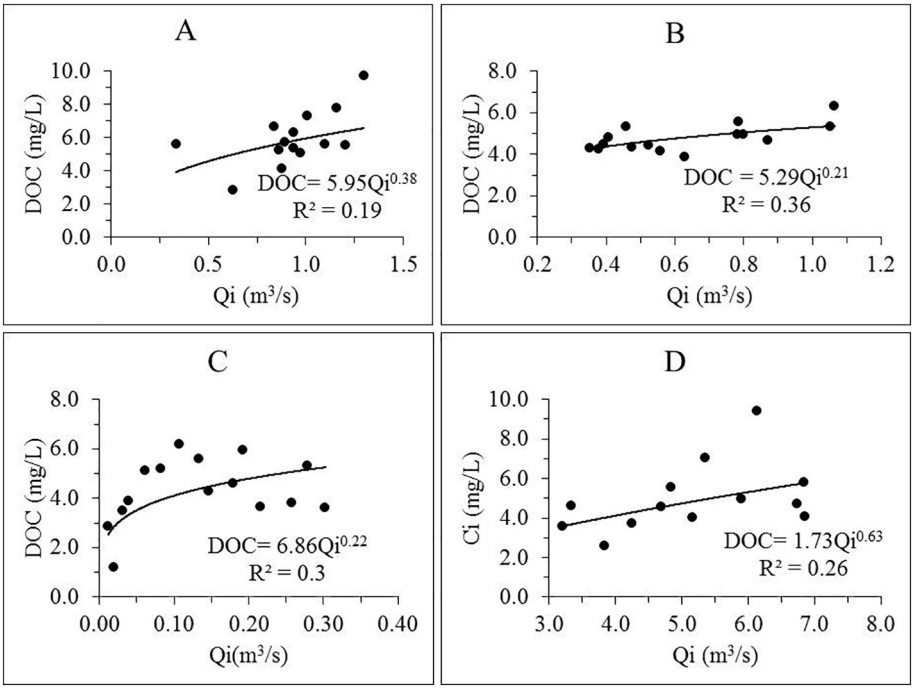


**Fig. 6.** Relationship between stream flow and DOC in the RRW. Letters A, B, C and D correspond to the streams at natural forest, tea, farm and outlet stations. Equations represent the power function of the relationship between discharge and stream DOC at the sites and the corresponding coefficient of determination ($R^2$).

**Table 1**
Annual and daily average DOC loading in in the RRW.

| Stream | Stream area[a] ($m^2$) | Stream DOC (mg/L) | Total flow ($m^3$) | Total DOC Load (t) | DOC load (t/day) | DOC load (t/day/$m^2$) |
|---|---|---|---|---|---|---|
| NF | 2.48 | 5.47 | 99,427,662.95 | 362.17 | 0.50 | 0.20 |
| Tea | 1.66 | 4.06 | 76,864,085.70 | 188.14 | 0.26 | 0.16 |
| Farm | 0.40 | 3.66 | 7,062,122.67 | 15.97 | 0.02 | 0.05 |
| Outlet | 8.33 | 5.73 | 286,538,549.94 | 1641.87 | 2.26 | 0.27 |

[a] The average cross section area calculated during discharge measurements using a mechanical current meter.

of the Rukarara River and in the streams. Table 1 presents annual and daily DOC loads site per site.

The table shows that daily DOC loads per unit area vary between locations of streams. The stream located in the natural forest exports higher amount of DOC than streams located in tea plantation and farming areas. Regarding the total DOC export for the whole watershed, the results show that there was a loss of 1641.87 t C at the outlet site for the period from March 2015 to February 2017 (Table 1), meaning an average of 820.94 t C every year. The DOC daily loss of the RRW was 2.26 t C and the annual DOC yield was 16.72 kg C/ha/year. Based on an estimate produced using the MODIS17A3 dataset of the period from 2000 to 2014 (ORNL DAAC, 2008), the mean daily NPP of the RRW was 26.79 t C. This indicates that the loss of DOC through riverine loading is 8.44% of the daily NPP within the watershed.

### 3.6. Spatial distribution of land use land cover

#### 3.6.1. LULC composition in the RRW

The classified image of the study area indicates that the LULC of the RRW is composed of agricultural land (42%), natural forest (32%), plantation forest (19%), barren and built up area (4%) and tea plantation (3%) (Fig. 7). The overall accuracy is 81.18%, whereas the Kappa coefficient is 0.76. Regarding the confusion matrix, the user and producer accuracies and the per-class Kappa indices are summarized in Tables 2 and 3.

#### 3.6.2. Spatial Indices of LULC classes

By decreasing order, estimated SI values are 15.85, 3.75, 2.63, 1.91and 1.75 respectively for tea plantations, tree plantation forest, natural forest, agriculture, and barren and built up areas. The tea plantation shows the highest SI, followed by the tree plantation forest. These results indicate that tea plantations are located in areas of the high drainage near the river or streams. The tea plantations class presumably has the highest SI because farmers want to sustain their production even in dry season and tend to grow tea close to drainage channels in less dry areas, and locate tea plantations accordingly. The farming area has low SI values because farmers use radical terraces that drain poorly. The barren and built up areas show the lowest SI essentially for the reason that they are established on smoothed out areas and therefore of very low drainage.

#### 3.6.3. Slope position and TWI distribution by LULC classes

The analysis indicated that slope positions and TWI values vary considerably between LULC classes. Summits and depressions are the two dominant slope positions in all LULC classes except in agriculture. In this class, summits and flat slopes dominate (Table 4).

The high slopes (defined as the slope positions from flat slopes to summits) are by increasing order: 64.40%, 63.75%, 56.47%, 53.77%, and 52.94% of the areas covered respectively by the natural forest, agriculture, tree plantation forest, bare and built up, and tea plantation classes. Considering the low slopes, tea and tree plantations and built up areas have the lowest slope positions and are therefore more preferentially located in valleys. These results show that more tea plantations, bare and built up areas and tree plantations are located in valleys, meaning in areas of overland flow collection. This tells us that these LULC classes could have a potentially positive effect on stream DOC loading.

The TWI values range from 5 to 17 with 8 as the index value that covers the biggest area in all LULC classes, except in the bare and built up class (Table 5). High and low TWI values cover areas within different LULC classes. Whereas the biggest area covered by high TWI values (11.39%) was found in tea plantations, the biggest area covered by low TWI values (83.38%) was found in bare and built up class. Regarding the ratio between high and low TWI values, the results indicate that it

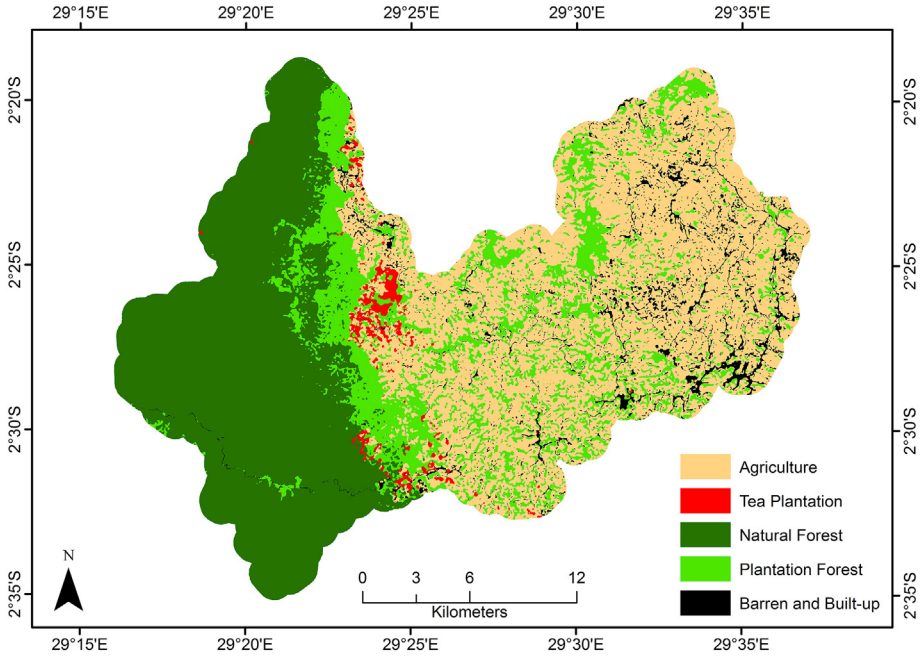


**Fig. 7.** LULC map of the RRW classified from a Rapid-Eye image obtained in June 2015. The land cover of the RRW is dominated by cropland, followed by natural forest, and tree plantation.

**Table 2**
Counts of training and evaluation sites and proportions of each LULC type. Training data are in columns; evaluation data in rows and proportions are in italic.

| LULC classes | Agriculture | Tea plantation | Natural forest | Bare and built up | Plantation forest | Total |
|---|---|---|---|---|---|---|
| Agriculture | 27 | 1 | 0 | 8 | 2 | 38 |
| | *0.16* | *0.01* | *0.00* | *0.05* | *0.01* | *0.22* |
| Tea plantation | 3 | 22 | 3 | 0 | 1 | 29 |
| | *0.02* | *0.13* | *0.02* | *0.00* | *0.01* | *0.17* |
| Natural forest | 0 | 1 | 18 | 0 | 2 | 21 |
| | *0.00* | *0.01* | *0.11* | *0.00* | *0.01* | *0.12* |
| Bare and Built up | 2 | 0 | 0 | 47 | 0 | 49 |
| | *0.01* | *0.00* | *0.00* | *0.28* | *0.00* | *0.29* |
| Plantation forest | 4 | 1 | 4 | 0 | 24 | 33 |
| | *0.02* | *0.01* | *0.02* | *0.00* | *0.14* | *0.19* |
| Total | 36 | 25 | 25 | 55 | 29 | 170 |
| | *0.21* | *0.15* | *0.15* | *0.32* | *0.17* | *1.00* |

varies between LULC classes. Tea plantations have the highest ratio (14.29%) followed by agriculture class (11.67%). This indicates that the tea plantation has the biggest saturated areas compared to other LULC classes within the RRW confirming their location in valleys as previously concluded.

*3.6.4. Time of concentration and lag time by LULC classes*

The $T_c$ (time of concentration) was estimated empirically using the Kerby-Kirpich method (Eqs. (10) and (11)) for five LULC classes (Fig. 7). The tea plantations and farm areas were however combined to make an agricultural land use land cover. The results indicated that the $T_c$ values varied between LULC classes. $T_c$ values range from 1.64 to 3.79 h with the longest time estimated for the natural forest and the lowest time for the agricultural areas (farm plus tea plantations) (Table 6). The corresponding lag time varied between 0.98 and 2.27 h. The results revealed that, within the RRW, the $T_d$ depends on flow path index. The natural forest (NF) showed the highest values of $T_c$ and $T_{lag}$, followed by the plantation forest (PF), the bare and built up areas (BBA) and agricultural lands (AGL). A second order polynomial regression fitted between $T_c$ values and the corresponding longest total flow lengths to the watershed outlet indicated a very strong correlation ($R^2 = 0.81$).

## 4. Discussion

*4.1. Between site and temporal variation of stream DOC*

Higher stream DOC was found at the natural forest site. This result is explained by the higher DOC in the soil of the natural forest, its high flow path index (Table 2), high TWI values (Table 5) and ridge-like topography in a 500 m buffer zone around the time of concentration sampling point. The large proportion of ridge topography around the sampling site suggests high overland and leakage flow into the stream. The high soil DOC is due to important accumulation of plant biomass in the natural forest, producing a high amount of soil organic carbon from which soil DOC is mobilized. High TWI and larger amounts of soil DOC can be taken together to explain the higher DOC in natural forest stream as compared to the other streams within the study area. These conditions lead to a more and less continuous transfer of soil DOC into natural forest streams through a leakage process. This is confirmed by the relatively low variation of stream DOC at the natural forest site as compared to the tea and farm sites.

*4.2. Response of stream DOC to stream flow volume*

All stream DOC values in the study area are responsive to stream flow volume. The overall b value for the RRW is higher than that of that for the natural forest and tea sites, indicating the influence of stream DOC concentrations contributed by other non-sampled streams within the RRW before reaching the Rukarara River outlet. In contrast, the overall *b* value for the RRW is less than that of the farm site. This implies the dilution of the level of concentration of DOC from the farm site stream when it reaches the Rukarara River.

Results indicated different streamflow contributions from quick flow and baseflow components within the RRW. Streams and large river were both characterized by important contributions from quick flow. The quick flow, direct response to rainfall events including overland flow or runoff, interflow and direct precipitation, transports dissolved matter such as DOC. This was confirmed by observations of increased stream DOC with increasing flow and decreased stream DOC with decreasing flow after the peak was reached for all sites (Fig. 6). These results imply both concentration and dilution effects. The dilution effect is attributed to the dissolution of DOC in the baseflow that increases due to rainfall. The concentration effect is attributed to the runoff, interflow and direct precipitation that mobilize and transport materials containing DOC into streams. Summarily, results indicate that the rate of flow is a key driver of the DOC concentration within the RRW: the stream DOC, and therefore its export, increases during the high flow periods.

*4.3. Impact of DOC loading on carbon sequestration in the RRW*

The DOC loss was estimated to be 8.43% of the daily average NPP of the RRW. Although the loss of DOC through loading was in low compared to the carbon net productivity, the observed DOC loss could have direct consequences for the net carbon balance in the watershed, and can constrain watershed productivity, as long as terrestrial ecosystems are the main source of stream DOC (Hinton et al., 1998). The carbon lost as DOC can affect the health of soils, exacerbating the study area degradation. As a product of incomplete decomposition of organic matter, DOC is favored in nutrient poor areas with limited decomposition, but with high C:N ratios (Mattsson et al., 2009; Clark et al., 2010). This tells us that any changes in riverine DOC export into streams can cause shifts in primary productivity, decomposition, leaching/discharges or transport in both terrestrial and aquatic ecosystems (Clark et al., 2010).

There are several factors that affect the DOC flux in the RRW, among them precipitation, deep percolation and translocation of organic matter through runoff. Key processes of stream DOC fluxes are terrestrial organic carbon production, its decomposition to DOC, leaching into the aquatic systems and transport into streams. LULC, soil properties, rainfall and topography influence the above-mentioned processes of DOC production and export. The positive relationship between DOC and

**Table 3**
User/producer accuracy and conditional Kappa.

| LULC classes | Producer accuracy (%) | Producer's conditional Kappa | User accuracy (%) | User's conditional Kappa |
|---|---|---|---|---|
| Agriculture | 75.00 | 0.70 | 71.05 | 0.65 |
| Tea plantation | 88.00 | 0.88 | 75.86 | 0.72 |
| Natural forest | 72.00 | 0.69 | 85.71 | 0.84 |
| Bare and built up | 85.45 | 0.79 | 95.92 | 0.94 |
| Plantation forest | 82.76 | 0.80 | 72.73 | 0.69 |

**Table 4**
Slope positions and covered areas by LULC classes within the RRW.

| Slope position | Natural forest (%) | Tree plantation forest (%) | Tea plantation (%) | Agriculture (%) | Bare and built up (%) |
|---|---|---|---|---|---|
| Summit | 29.89 | 42.23 | 41.13 | 23.86 | 51.17 |
| Upper slope | 12.35 | 4.91 | 3.44 | 13.51 | 0.78 |
| Midslope | 2.91 | 1.39 | 1.07 | 3.16 | 0.14 |
| Flat slope | 19.24 | 7.95 | 7.30 | 23.23 | 1.68 |
| Lower slope | 10.38 | 3.76 | 4.62 | 12.46 | 0.86 |
| Depression | 25.22 | 39.77 | 42.44 | 23.79 | 45.37 |
| High slopes | 64.40 | 56.47 | 52.94 | 63.75 | 53.77 |
| Low slopes | 35.60 | 43.53 | 47.06 | 36.25 | 46.33 |

water flow indicates that the hydrology of the watershed plays a big role in DOC mobilization and export in the RRW.

### 4.4. Impact of land use land cover change on time of concentration of stream DOC

The results of $T_c$ indicate that $T_c$ values vary per LULC class. This tells us that changes in LULC within the RRW can impact the $T_c$ values, and therefore stream DOC loads depending on involved land cover type. The conversion of land cover types with high Kerby coefficients into types with low Kerby coefficients, for example, the conversion of natural forest into agricultural lands or settlements, can reduce the time of concentration. On the contrary, the conversion of land cover types with low Kerby coefficients into types with high Kerby coefficient, for example, from small farming into forest plantations, could increase the $T_c$. A decrease of land cover intensity by the conversion of forests into agricultural lands could increase the intensity of runoff process and therefore the export of solutes, including DOC, into streams. This can be associated with an increase of rainfall within the RRW due to climate change; there is thus a risk of an increase in stream DOC in the coming future. Regional projection climate models indicate that within the RRW, rainfall is expected to increase about 10% by 2050 (Warnest et al., 2012). If the relationship between DOC concentration and water flow remains consistent, the DOC would proportionally increase in the future. This increase of DOC in the Rukarara River and its tributaries can affect its water quality, metabolism, and nutrient uptake, bioavailability of toxic compounds, microorganism growth, and biodiversity.

Low values of $T_c$ and $T_{lag}$ demonstrate that, in case of torrential rainfall, accelerated flow and water concentration within the RRW would cause a rapid transmission of the flood wave from uphill to downstream, and an exponential growth of the discharge in a short time. This would lead to increased export of DOC into stream waters.

### 4.5. Comparison of DOC in the RRW to other sites

The DOC concentration in the RRW was equal to or higher than DOC concentration previously found in both temperate and tropical watersheds. For the case of temperate watersheds, the RRW concentration was equal to or higher than that found in the Embarras River within a row-cropland watershed in Illinois (1–18 mg C/L) (Royer and David, 2005); 0.15 to 15.97 mg C/L in the Kings Creek grassland watershed (Rüegg et al., 2015), in the Colorado River in the Rocky Mountains (1.0–6.9 mg C/L) (Miller, 2012); and in small mountainous rivers of the North and South Islands of New Zealand (<0.1–4.0 mg C/L) (Carey et al., 2005). In tropical watersheds, the DOC values from this study were equal to or higher than those in the small mountainous rivers in the Luquillo Experimental Forest at Puerto Rico (1.32–2.16 mg C/L) (McDowell and Asbury, 1994); in the Basse-Terre Island watersheds in Guadeloupe (0.52–7.22 mg C/L) (Lloret et al., 2013), and in the Oubangui, a major tributary of the Congo River (1–6 mg C/L) (Bouillon et al., 2014).

Regarding the DOC flux and yield in the RRW, the DOC flux was lower than that in tropical Africa ($2.80 * 10^{13}$ g C/y), the Americas ($5.82 * 10^{13}$ g C/y), Asia ($4.50 * 10^{13}$ g C/y) and Oceania ($4.48 * 10^{12}$ g C/y) (Huang et al., 2012). The DOC yield in the RRW (16.73 kg C/ha/year or 1.67 g C/m$^2$/year) was equal to or higher than that ones in the Kings Creek watershed (0.29 kg C/ha/year) (Rüegg et al., 2015), in tropical large rivers of Africa (1 g C/m$^2$/year), Oceania (0.76 g C/m$^2$/year) (Huang, 2012), and the global DOC yield (1.38–1.44 g C/m$^2$/year) (Huang, 2012). On the contrary, the DOC yield in the RRW was equal to or lower to those ones found in row-crop watersheds in Illinois (3–23 kg C/ha/year) (Royer and David, 2005), in tropical rivers of Americas (3.16 g C/m$^2$/year), and Asia (3.97 g C/m$^2$/year), total tropical area (2.13 g C/m$^2$/year) (Huang, 2012), Panamanian rivers (2.29–7.97 t/km$^2$/y) (Goldsmith et al., 2015), Guadeloupe (2.5–5.7 t C/km$^2$/year) (Lloret et al., 2013).

Waters from tropical rain forests are carbon-rich "black water" systems. Headstreams export up 90% of the total annual carbon in these tropical waters (Leach et al., 2016). The high DOC concentration in the RRW is extorped up by its headstreams originating from Nyungwe rainforest. This forest, as other tropical forest close to Equator, has high rate of NPP, ample rainfall and sunlight, warm temperatures, and long growing seasons (Cleveland et al., 2013). The RRW ($2^0$20′S–$02^0$35′S) is among those ecosystems with high rate of NPP (1108 ± 120 g C m$^{-2}$ yr$^{-1}$) (Huang, 2012). This high NPP is a result of the amount of solar radiation available in those ecosystems. High rate of NPP associated to ample rainfall and sunlight, warm temperatures, and long growing seasons, may explain high DOC concentration, flux and yield in the RRW compared to riverine DOC values in temperate watersheds. The high NPP reflects ability to produce great amount of

**Table 5**
Range and distribution of Topographic Wetness Index (TWI) by LULC within the RRW in May 2015.

| LULC classes | TWI range | High TWI (%) | Low TWI (%) | High and low TWI ratio (%) |
|---|---|---|---|---|
| Agriculture | 6 -7 | 8.61 | 73.75 | 11.67 |
| Tea plantation | 6 -15 | 11.39 | 79.73 | 14.29 |
| Natural forest | 6 -16 | 8.76 | 83.01 | 10.56 |
| Bare and Built up | 6 -17 | 4.78 | 83.38 | 5.73 |
| Tree plantation forest | 5 -17 | 6.27 | 77.46 | 8.09 |

**Table 6**
Time of concentration and lag time for LULC classes in the RRW.

| LULC | Altitude (m) | SFL (m) | PFL (m) | FLE (m) | S (dim.) | $T_{ov}$ (h) | $T_{ch}$ (h) | $T_c$ (h) | Tlag (h) |
|---|---|---|---|---|---|---|---|---|---|
| NF | 2048 -2925 | 8456 | 9902 | 18358 | 0.103 | 2.52 | 1.27 | 3.79 | 2.27 |
| AGL | 1542 -2788 | 4513 | 5095 | 9608 | 0.130 | 1.13 | 0.51 | 1.64 | 0.98 |
| PF | 1542 -2596 | 8672 | 4669 | 13341 | 0.092 | 2.29 | 0.54 | 2.83 | 1.70 |
| BBA | 1542 -2768 | 5856 | 9902 | 15758 | 0.067 | 1.48 | 1.10 | 2.58 | 1.55 |

*SFL*: secondary longest flow length; *PFL*: primary flow length; *FLE*: longest flow length to watershed exit; *dim.*: dimensionless; $T_{ov}$: overland time of concentration; $T_{ch}$: channel time of concentration; NF: natural forest; AGL: agriculture area; PF: plantation forest; BBA: bare and built up area.

organic carbon that is transformed into soil DOC by microbial communities. Warm temperature, by accelerating decomposition and mineralization of organic matter, positively impact on soil DOC production (Worrall et al., 2003). Ample rainfall alters water budget and discharge and positively impact on DOC export into the RRW through runoff and leaching processes. Thus, hydrologic regime is an important factor in controlling DOC concentrations and flux in the RRW and other similar tropical watersheds. The DOC flux in the RRW and comparable watersheds may be enhanced by the steep slopes and the inability of their highly weathered soils to adsorb DOC (St John and Anderson, 1982).

Local variations in rates of organic carbon production, accumulation, turnover, decomposition and export may explain the difference between DOC values in the RRW and other tropical watersheds. Such variations comprise local differences in vegetation, hydrology, topography, climate, soil properties, soil temperature and moisture, altitude; land management, atmospheric $CO_2$, mineral soil absorption, dry-wet cycle of hydrological conditions, nitrogen saturation, and surface and subsurface runoff (Yang, 2013; Olefeldt et al., 2012; Williams et al., 2010; Zhu et al., 2010; Mattsson et al., 2009). For example, vegetation in the Basse-Terre Island watersheds and in the RRW is similar but the two ecosystems differ by their annual rainfall. Rainfall in the RRW (1300 to 1450 mm) is relatively less important in the RRW than in the Basse-Terre Island watersheds in Guadeloupe (1200 to 8000 mm $year^{-1}$) (Lloret et al., 2013). This difference may explain the difference in riverine DOC values in rivers within these two comparable ecosystems. High DOC values in rivers of Guadeloupe may be explained by heavy rainfall resulting in more important runoff compared to the RRW and therefore more important lateral transfer of DOC into waters. Heavy rainfall may also leach more amounts of DOC, from the vegetation and soils, in the Guadeloupe than in the RRW.

## 5. Conclusions

In this paper, we have investigated on dynamics of stream DOC in the Rukarara River Watershed in Rwanda. The analysis of between site variations of the stream DOC revealed that stream DOC concentration differs significantly between natural forest, tea plantation and farm sites. The stream DOC is positively influenced by land use and land cover, and consequently any change in the land could potentially impact stream DOC. Compared to other watersheds, the RRW showed DOC concentration, flux and yield that were equal to, lower or higher than DOC values previously found in both temperate and tropical watersheds.

Stream DOC was sensitive to stream water flow volume, but the stream at the natural forest site showed the highest sensitivity. The lowest sensitivity of stream DOC to stream water flow volume was observed in the stream in the farm areas. Stream DOC increases with stream flow volume and hence any change in stream flow volume controlling factors such as precipitation, temperature and sedimentation, could affect stream DOC concentration in the Rukarara River Watershed.

The main source of stream DOC was the quick flow at all sites. As a consequence, any change in runoff, interflow and dissolved carbon in precipitation could affect contents of stream DOC in the Rukarara River Watershed. Land use and land cover also influences stream DOC loading. During the study period, the annual DOC load and daily DOC load per unit area were found to be higher for the stream at the natural forest site than at other sites. The loss of carbon in the form of DOC was essentially due to quick flow in both agricultural areas and natural forest. But tea plantations may play an important role in DOC loading; they were found to have the highest spatial index, lower slopes, the highest ratio between high and low TWI, and the lowest time of concentration and lag time. An increased DOC export may degrade both terrestrial and aquatic ecosystems within the Rukarara watershed. Estimates of water DOC loading are therefore useful information in planning and management of both water and land resources in the watershed for its productivity and sustainable conservation.

## Acknowledgements

The authors would like to thank the University of Rwanda and the Sida Partnership Program for the financial support of this work. The MOD17A3 data product was retrieved from the NASA Land Processes Distributed Active Archive Center (LP DAAC), USGS/Earth Resources Observation and Science (EROS) Center, Oak Ridge, Tennessee, USA, https://daac.ornl.gov/modiswebservice.

## References

Alvarez-Cobelas, M., Angeler, D.G., Sánchez-Carrillo, S., Almendros, G., 2012. A worldwide view of organic carbon export from catchments. Biogeochemistry 107 (1–3): 275–293. https://doi.org/10.1007/s10533-010-9553-z.

Amon, R.M., Meon, B., 2004. The biogeochemistry of dissolved organic matter and nutrients in two large Arctic estuaries and potential implications for our understanding of the Arctic Ocean system. Mar. Chem. 92 (1):311–330. https://doi.org/10.1016/j.marchem.2004.06.034.

Aufdenkampe, A.K., Mayorga, E., Raymond, P.A., Melack, J.M., Doney, S.C., Alin, S.R., ... Yoo, K., 2011. Riverine coupling of biogeochemical cycles between land, oceans, and atmosphere. Front. Ecol. Environ. 9 (1). https://doi.org/10.1890/100014.

Baldassarre, G.D., Montanari, A., 2009. Uncertainty in river discharge observations: a quantitative analysis. Hydrol. Earth Syst. Sci. 13 (6):913–921. https://doi.org/10.5194/hess-13-913-2009.

Battin, T.J., Luyssaert, S., Kaplan, L.A., Aufdenkampe, A.K., Richter, A., Tranvik, L.J., 2009. The boundless carbon cycle. Nat. Geosci. 2 (9):598–600. https://doi.org/10.1038/ngeo618.

Berberoglu, S., Curran, P.J., 2004. Merging spectral and textural information for classifying remotely sensed images. Remote Sensing Image Analysis: Including the Spatial Domain. Springer, Netherlands:pp. 113–136 https://doi.org/10.1007/978-1-4020-2560-0_7.

Beven, K.J., Kirkby, M.J., 1979. A physically based variable contributing area model of basin hydrology. Hydrol. Sci. Bull. 24:43–69. https://doi.org/10.1080/02626667909491834.

Bouillon, S., Yambélé, A., Gillikin, D.P., Teodoru, C., Darchambeau, F., Lambert, T., Borges, A.V., 2014. Contrasting biogeochemical characteristics of the Oubangui River and tributaries (Congo River basin). Sci. Rep. 4 (5402). https://doi.org/10.1038/srep05402.

Brodie, R.S., Hostetler, S., 2005, November. A review of techniques for analysing baseflow from stream hydrographs. Proceedings of the NZHS-IAH-NZSSS 2005 Conference. vol. 28 (Auckland New Zealand).

Carey, A.E., Gardner, C.B., Goldsmith, S.T., Lyons, W.B., Hicks, D.M., 2005. Organic carbon yields from small, mountainous rivers, New Zealand. Geophys. Res. Lett. 32 (15). https://doi.org/10.1029/2005GL023159.

Cassidy, R., Jordan, P., 2011. Limitations of instantaneous water quality sampling in surface-water catchments: comparison with near-continuous phosphorus time-series data. J. Hydrol. 405 (1):182–193. https://doi.org/10.1016/j.jhydrol.2011.05.020.

Chin, D.A., Mazumdar, A., Roy, P.K., 2000. Water-resources Engineering. vol. 12. Prentice Hall, Englewood Cliffs.

Clark, J.M., Bottrell, S.H., Evans, C.D., Monteith, D.T., Bartlett, R., Rose, R., ... Chapman, P.J., 2010. The importance of the relationship between scale and process in understanding long-term DOC dynamics. Sci. Total Environ. 408 (13):2768–2775. https://doi.org/10.1016/j.scitotenv.2010.02.046.

Cleveland, C.C., Houlton, B.Z., Smith, W.K., Marklein, A.R., Reed, S.C., Parton, W., ... Running, S.W., 2013. Patterns of new versus recycled primary production in the terrestrial biosphere. Proc. Natl. Acad. Sci. 110 (31):12733–12737. https://doi.org/10.1073/pnas.1302768110.

Cohen, J., 1960. A coefficient of agreement for nominal scales. Educ. Psychol. Meas. 20 (1): 37–46. https://doi.org/10.1177/001316446002000104.

Cole, J.J., Prairie, Y.T., Caraco, N.F., McDowell, W.H., Tranvik, L.J., Striegl, R.G., ... Melack, J., 2007. Plumbing the global carbon cycle: integrating inland waters into the terrestrial carbon budget. Ecosystems 10 (1):172–185. https://doi.org/10.1007/s10021-006-9013-8.

Congalton, R.G., Green, K., 2008. Assessing the Accuracy of Remotely Sensed Data: Principles and Practices. CRC Press https://doi.org/10.1201/9781420055139.

Costache, R., 2014. Using GIS techniques for assessing lag time and concentration time in small river basins. Case study: Pecineaga river basin, Romania. Geogr. Tech. 9 (1), 31–38.

Delpla, I., Jung, A.V., Baures, E., Clement, M., Thomas, O., 2009. Impacts of climate change on surface water quality in relation to drinking water production. Environ. Int. 35 (8): 1225–1233. https://doi.org/10.1016/j.envint.2009.07.001.

Deumlich, D., Schmidt, R., Sommer, M., 2010. A multiscale soil–landform relationship in the glacial-drift area based on digital terrain analysis and soil attributes. J. Plant Nutr. Soil Sci. 173 (6):843–851. https://doi.org/10.1002/jpln.200900094.

DHI, M., 2011. 11–A Modelling System for Rivers and Channels, Reference Manual. DHI Water & Environment, Denmark.

Dingman, S.L., 1984. Fluvial Hydrology.

Dingman, S.L., 2008. Physical Hydrology. Second ed. Waveland Press, Incorporated, University of Hampshire.

Elwan, A., Singh, R., Horne, D., Roygard, J., Clothier, B., 2015. Nitrogen attenuation factor: can it tell a story about the journey of nutrients in different subsurface environments? Moving Farm Systems to Improved Attenuation

Erlandsson, M., Cory, N., Fölster, J., Köhler, S., Laudon, H., Weyhenmeyer, G.A., Bishop, K., 2011. Increasing dissolved organic carbon redefines the extent of surface water acidification and helps resolve a classic controversy. Bioscience 61 (8):614–618. https://doi.org/10.1525/bio.2011.61.8.7.

Evans, C.D., Monteith, D.T., Cooper, D.M., 2005. Long-term increases in surface water dissolved organic carbon: observations, possible causes and environmental impacts. Environ. Pollut. 137 (1):55–71. https://doi.org/10.1016/j.envpol.2004.12.031.

Evans, J.S., Oakleaf, J., Cushman, S.A., Theobald, D., 2014. An ArcGIS Toolbox for Surface Gradient and Geomorphometric Modeling, Version 2.0-0. Laramie, WY. http://evansmurphy.wix.com/evansspatial.

Fedorko, E., 2012. Spatial distribution of land type in regression models of pollutant loading. J. Spat. Hydrol. 5 (2).

Fernández-Pérez, M., Flores-Céspedes, F., González-Pradas, E., Ure-a-Amate, M.D., Villafranca-Sánchez, M., Socías-Viciana, M., Pérez-García, S., 2005. Effects of dissolved organic carbon on phosphate retention on two calcareous soils. J. Agric. Food Chem. 53 (1):84–89. https://doi.org/10.1021/jf048767o.

Findlay, S., Quinn, J.M., Hickey, C.W., Burrell, G., Downes, M., 2001. Effects of land use and riparian flowpath on delivery of dissolved organic carbon to streams. Limnol. Oceanogr. 46 (2):345–355. https://doi.org/10.4319/lo.2001.46.2.0345.

Fowler, D., Smith, R.I., Muller, J.B.A., Hayman, G., Vincent, K.J., 2005. Changes in the atmospheric deposition of acidifying compounds in the UK between 1986 and 2001. Environ. Pollut. 137 (1):15–25. https://doi.org/10.1016/j.envpol.2004.12.028.

Freeman, C., Evans, C.D., Monteith, D.T., Reynolds, B., Fenner, N., 2001. Export of organic carbon from peat soils. Nature 412 (6849), 785.

Freeman, C., Fenner, N., Ostle, N.J., Kang, H., Dowrick, D.J., Reynolds, B., ... Hudson, J., 2004. Export of dissolved organic carbon from peatlands under elevated carbon dioxide levels. Nature 430 (6996):195–198. https://doi.org/10.1038/nature02707.

Garg, J., Garg, H.K., 2001. Water quality management strategies for conservation of Bhopal waters. Environ. Conserv. J. 2 (2), 101–104.

Goldsmith, S.T., Lyons, W.B., Harmon, R.S., Harmon, B.A., Carey, A.E., McElwee, G.T., 2015. Organic carbon concentrations and transport in small mountain rivers, Panama. Appl. Geochem. 63:540–549. https://doi.org/10.1007/s11802-009-0352-x.

Gu, D., Zhang, L., Jiang, L., 2009. The effects of estuarine processes on the fluxes of inorganic and organic carbon in the Yellow River estuary. J. Ocean Univ. China 8 (4): 352–358. https://doi.org/10.1007/s11802-009-0352-x.

Harrison, A.F., Taylor, K., Scott, A., Poskitt, J.A.N., Benham, D., Grace, J., ... Rowland, P., 2008. Potential effects of climate change on DOC release from three different soil types on the Northern Pennines UK: examination using field manipulation experiments. Glob. Chang. Biol. 14 (3):687–702. https://doi.org/10.1111/j.1365-2486.2007.01504.x.

Hinton, M.J., Schiff, S.L., English, M.C., 1998. Sources and flowpaths of dissolved organic carbon during storms in two forested watersheds of the Precambrian Shield. Biogeochemistry 41 (2), 175–197.

Hongve, D., Riise, G., Kristiansen, J.F., 2004. Increased colour and organic acid concentrations in Norwegian forest lakes and drinking water–a result of increased precipitation? Aquat. Sci. 66 (2):231–238. https://doi.org/10.1007/s00027-004-0708-7.

Hove, H., Parry, J.E., Lujara, N., 2010. Maintenance of Hydropower Potential in Rwanda Through Ecosystem Restoration. World Resources Report, Washington DC Available online at. http://www.worldresourcesreport.org.

Huang, T.H., Fu, Y.H., Pan, P.Y., Chen, C.T.A., 2012. Fluvial carbon fluxes in tropical rivers. Curr. Opin. Environ. Sustain. 4 (2):162–169. https://doi.org/10.1016/j.cosust.2012.02.004.

Janssen, L.L.F., Van der Wel, F.J.M., 1994. Accuracy assessment of satellite derived land-cover data: a review. Photogrammeric Remote Sens. 60, 419–426.

Jawitz, J.W., Mitchell, J., 2011. Temporal inequality in catchment discharge and solute export. Water Resour. Res. 47 (10). https://doi.org/10.1029/2010WR010197.

Johnson, M.S., Lehmann, J., Couto, E.G., Novaes Filho, J.P., Riha, S.J., 2006. DOC and DIC in flowpaths of Amazonian headwater catchments with hydrologically contrasting soils. Biogeochemistry 81 (1), 45–57.

Kane, E.S., Mazzoleni, L.R., Kratz, C.J., Hribljan, J.A., Johnson, C.P., Pypker, T.G., Chimner, R., 2014. Peat porewater dissolved organic carbon concentration and lability increase with warming: a field temperature manipulation experiment in a poor-fen. Biogeochemistry 119 (1–3):161–178. https://doi.org/10.1007/s10533-014-9955-4.

Kavzoglu, T., Mather, P.M., 2003. The use of back propagating artificial neural networks in land cover classification. Int. J. Remote Sens. 24 (23):4907–4938. https://doi.org/10.1080/0143116031000114851.

Lambert, T., Darchambeau, F., Bouillon, S., Alhou, B., Mbega, J.D., Teodoru, C.R., ... Borges, A.V., 2015. Landscape control on the spatial and temporal variability of chromophoric dissolved organic matter and dissolved organic carbon in large African rivers. Ecosystems 18 (7):1224–1239. https://doi.org/10.1007/s10021-015-9894-5.

Laraque, A., Castellanos, B., Steiger, J., Lòpez, J.L., Pandi, A., Rodriguez, M., ... Lagane, C., 2013. A comparison of the suspended and dissolved matter dynamics of two large inter-tropical rivers draining into the Atlantic Ocean: the Congo and the Orinoco. Hydrol. Process. 27 (15):2153–2170. https://doi.org/10.1002/hyp.9776.

Leach, J.A., Larsson, A., Wallin, M.B., Nilsson, M.B., Laudon, H., 2016. Twelve year interannual and seasonal variability of stream carbon export from a boreal peatland catchment. J. Geophys. Res.: Biogeosci. 121 (7), 1851–1866.

Legates, D.R., McCabe, G.J., 1999. Evaluating the use of "goodness-of-fit" measures in hydrologic and hydroclimatic model validation. Water Resour. Res. 35 (1):233–241. https://doi.org/10.1029/1998WR900018.

Li, M., Shao, Q., Zhang, L., Chiew, F.H., 2010. A new regionalization approach and its application to predict flow duration curve in ungauged basins. J. Hydrol. 389 (1–2), 137–145.

Littlewood, I.G., Watts, C.D., Custance, J.M., 1998. Systematic application of United Kingdom river flow and quality databases for estimating annual river mass loads (1975–1994). Sci. Total Environ. 210:21–40. https://doi.org/10.1016/S0048-9697(98)00042-4.

Lloret, E., Dessert, C., Pastor, L., Lajeunesse, E., Crispi, O., Gaillardet, J., Benedetti, M.F., 2013. Dynamic of particulate and dissolved organic carbon in small volcanic mountainous tropical watersheds. Chem. Geol. 351:229–244. https://doi.org/10.1016/j.chemgeo.2013.05.023.

Lyne, V., Hollick, M., 1979, September. Stochastic time-variable rainfall-runoff modelling. Institute of Engineers Australia National Conference. vol. 1979, pp. 89–93.

Mattsson, T., Kortelainen, P., Laubel, A., Evans, D., Pujo-Pay, M., Räike, A., Conan, P., 2009. Export of dissolved organic matter in relation to land use along a European climatic gradient. Sci. Total Environ. 407 (6):1967–1976. https://doi.org/10.1016/j.scitotenv.2008.11.014.

McDowell, W.H., Asbury, C.E., 1994. Export of carbon, nitrogen, and major ions from three tropical montane watersheds. Limnol. Oceanogr. 39 (1), 111–125.

Miller, M.P., 2012. The influence of reservoirs, climate, land use and hydrologic conditions on loads and chemical quality of dissolved organic carbon in the Colorado River. Water Resour. Res. 48 (12). https://doi.org/10.1029/2012WR012312.

Monteith, J.L., 1972. Solar radiation and productivity in tropical ecosystems. J. Appl. Ecol. 9 (3), 747–766.

Monteith, D.T., Evans, C.D., Henrys, P.A., Simpson, G.L., Malcolm, I.A., 2014. Trends in the hydrochemistry of acid-sensitive surface waters in the UK 1988–2008. Ecol. Indic. 37:287–303. https://doi.org/10.1016/j.ecolind.2012.08.013.

Moore, I.D., Grayson, R.B., Ladson, A.R., 1991. Digital terrain modelling: a review of hydrological, geomorphological, and biological applications. Hydrol. Process. 5 (1):3–30. https://doi.org/10.1002/hyp.3360050103.

Moquet, J.S., Guyot, J.L., Crave, A., Viers, J., Filizola, N., Martinez, J.M., ... Noriega, L., 2016. Amazon River dissolved load: temporal dynamics and annual budget from the Andes to the ocean. Environ. Sci. Pollut. Res. 23 (12):11405–11429. https://doi.org/10.1007/s11356-015-5503-6.

Moriasi, D.N., Arnold, J.G., Van Liew, M.W., Bingner, R.L., Harmel, R.D., Veith, T.L., 2007. Model evaluation guidelines for systematic quantification of accuracy in watershed simulations. Trans. ASABE 50 (3):885–900. https://doi.org/10.13031/2013.23153.

Munson, R.K., Gherini, S.A., 1993. Influence of organic acids on the pH and acid-neutralizing capacity of Adirondack Lakes. Water Resour. Res. 29 (4):891–899. https://doi.org/10.1029/92WR02328.

Nash, J.E., Sutcliffe, J.V., 1970. River flow forecasting through conceptual models part I—a discussion of principles. J. Hydrol. 10 (3):282–290. https://doi.org/10.1016/0022-1694(70)90255-6.

Olefeldt, D., Roulet, N., Giesler, R., Persson, A., 2012. Total waterborne carbon export and DOC composition from ten nested subarctic peatland catchments: importance of peatland cover, groundwater influence, and inter-annual variability of precipitation patterns. Hydrol. Process. https://doi.org/10.1002/hyp.9358.

ORNL DAAC, 2008. MODIS Collection 5 Land Products Global Subsetting and Visualization Tool. ORNL DAAC, Oak Ridge, Tennessee, USA. Accessed April 21, 2017. Subset Obtained for MOD17A3 Product at 2S, 29.9E, Time Period: 2000-01-01 to 2014-12-31, and Subset Size: 201 × 201 km. https://doi.org/10.3334/ORNLDAAC/1241.

Paeth, H., Born, K., Girmes, R., Podzun, R., Jacob, D., 2009. Regional climate change in tropical and northern Africa due to greenhouse forcing and land use changes. J. Clim. 22 (1):114–132. https://doi.org/10.1175/2008JCLI2390.1.

Pagano, T., Bida, M., Kenny, J.E., 2014. Trends in levels of allochthonous dissolved organic carbon in natural water: a review of potential mechanisms under a changing climate. Water 6 (10):2862–2897. https://doi.org/10.3390/w6102862.

Palviainen, M., Laurén, A., Launiainen, S., Piirainen, S., 2016. Predicting the export and concentrations of organic carbon, nitrogen and phosphorus in boreal lakes by catchment characteristics and land use: a practical approach. Ambio:1–13 https://doi.org/10.1007/s13280-016-0789-2.

Post, E., Forchhammer, M.C., Bret-Harte, M.S., Callaghan, T.V., Christensen, T.R., Elberling, B., ... Ims, R.A., 2009. Ecological dynamics across the Arctic associated with recent climate change. Science 325 (5946):1355–1358. https://doi.org/10.1126/science.1173113.

Prairie, Y.T., 2008. Carbocentric limnology: looking back, looking forward. Can. J. Fish. Aquat. Sci. 65 (3):543–548. https://doi.org/10.1139/f08-011.

Qiu, F., Jensen, J.R., 2004. Opening the black box of neural networks for remote sensing image classification. Int. J. Remote Sens. 25 (9):1749–1768. https://doi.org/10.1080/01431160310001618798.

Ren, W., Tian, H., Cai, W.J., Lohrenz, S.E., Hopkinson, C.S., Huang, W.J., ... He, R., 2016. Century-long increasing trend and variability of dissolved organic carbon export from the Mississippi River basin driven by natural and anthropogenic forcing. Glob. Biogeochem. Cycles 30 (9):1288–1299. https://doi.org/10.1002/2016GB005395.

Rossiter, D.G., 2004. Statistical methods for accuracy assessment of classified thematic maps. Technical Note. International Institute for Geo-information Science & Earth Observation (ITC), Enschede.

Roussel, M.C., Thompson, D.B., Fang, X., Cleveland, T.G., Garcia, C.A., 2005. Time-parameter Estimation for Applicable Texas Watersheds. Department of Civil Engineering, Lamar University, Beaumont, TX, USA.

Rowe, E.C., Tipping, E., Posch, M., Oulehle, F., Cooper, D.M., Jones, T.G., ... Evans, C.D., 2014. Predicting nitrogen and acidity effects on long-term dynamics of dissolved organic matter. Environ. Pollut. 184:271–282. https://doi.org/10.1016/j.envpol.2013.08.023.

Royer, T.V., David, M.B., 2005. Export of dissolved organic carbon from agricultural streams in Illinois, USA. Aquat. Sci. 67 (4):465–471. https://doi.org/10.1007/s00027-005-0781-6.

Rüegg, J., Eichmiller, J.J., Mladenov, N., Dodds, W.K., 2015. Dissolved organic carbon concentration and flux in a grassland stream: spatial and temporal patterns and processes from long-term data. Biogeochemistry 125 (3):393–408. https://doi.org/10.1007/s10533-015-0134-z.

Salimon, C., dos Santos Sousa, E., Alin, S.R., Krusche, A.V., Ballester, M.V., 2013. Seasonal variation in dissolved carbon concentrations and fluxes in the upper Purus River,

southwestern Amazon. Biogeochemistry 114 (1–3):245–254. https://doi.org/10.1007/s10533-012-9806-0.
SanClements, M.D., Oelsner, G.P., McKnight, D.M., Stoddard, J.L., Nelson, S.J., 2012. New insights into the source of decadal increases of dissolved organic matter in acid-sensitive lakes of the northeastern United States. Environ. Sci. Technol. 46: 3212–3219. https://doi.org/10.1021/es204321x.
Singh, N.K., Reyes, W.M., Bernhardt, E.S., Bhattacharya, R., Meyer, J.L., Knoepp, J.D., Emanuel, R.E., 2016. Hydro-climatological influences on long-term dissolved organic carbon in a mountain stream of the southeastern United States. J. Environ. Qual. https://doi.org/10.2134/jeq2015.10.0537.
Spencer, R.G., Butler, K.D., Aiken, G.R., 2012. Dissolved organic carbon and chromophoric dissolved organic matter properties of rivers in the USA. J. Geophys. Res. Biogeosci. 117 (G3). https://doi.org/10.1029/2011JG001928.
St John, T.V., Anderson, A.B., 1982. A re-examination of plant phenolics as a source of tropical black water rivers. Trop. Ecol. 23, 151–154.
Stanley, E.H., Powers, S.M., Lottig, N.R., Buffam, I., Crawford, J.T., 2012. On temporary changes in dissolved organic carbon (DOC) in human-dominated rivers: is there a role for DOC management? Freshw. Biol. 57 (s1):26–42. https://doi.org/10.1111/j.1365-2427.2011.02613.x.
Stedmon, C.A., Amon, R.M.W., Rinehart, A.J., Walker, S.A., 2011. The supply and characteristics of colored dissolved organic matter (CDOM) in the Arctic Ocean: pan Arctic trends and differences. Mar. Chem. 124 (1):108–118. https://doi.org/10.1016/j.marchem.2010.12.007.
Sucker, C., Krause, K., 2010. Increasing dissolved organic carbon concentrations in freshwaters: what is the actual driver? iFor.-Biogeosci. For. 3 (4):106–108. https://doi.org/10.3832/ifor0546-003.
Wanielista, Kersten, R., Eaglin, R., 1997. Hydrology Water Quantity and Quality Control. 2nd ed. John Wiley & Sons.
Warnest, M., Sagashya, G., Nkurunzinza, E., 2012. Emerging in a Changing Climate – Sustainable Land Use Management in Rwanda. FIG (International Federation of surveyors).
Welderufael, W.A., Woyessa, Y.E., 2009. Stream flow analysis and comparison of methods for base flow separation: case study of the Modder River basin in central South Africa. Interim: Interdiscip. J. 8 (2), 107–119.
Wetzel, R.G., 2001. Limnology: Lake and River Ecosystems. Gulf Professional Publishing.
Williams, C.J., Yamashita, Y., Wilson, H.F., Jaffé, R., Xenopoulos, M.A., 2010. Unraveling the role of land use and microbial activity in shaping dissolved organic matter characteristics in stream ecosystems. Limnol. Oceanogr. 55 (3):1159–1171. https://doi.org/10.4319/lo.2010.55.3.1159.
Worrall, F., Burt, T.P., 2008. The effect of severe drought on the dissolved organic carbon (DOC) concentration and flux from British rivers. J. Hydrol. 361 (3):262–274. https://doi.org/10.1016/j.jhydrol.2008.07.051.
Worrall, F., Reed, M., Warburton, J., Burt, T., 2003. Carbon budget for a British upland peat catchment. Sci. Total Environ. 312 (1):133–146. https://doi.org/10.1016/S0048-9697(03)00226-2.
Yang, Y., 2013. Studying Soil Moisture and Land-to-Water Carbon Export in Urbanized Coastal Areas Using Remotely Sensed Data and a Regional Hydro-ecological Model. University of Massachusetts Boston.
Zhu, Z., Bergamaschi, B., Bernknopf, R., Clow, D., Dye, D., Faulkner, S., ... Wein, A., 2010. Public review draft—a method for assessing carbon stocks, carbon sequestration, and greenhouse-gas fluxes in ecosystems of the United States under present conditions and future scenarios. US Geol. Sci. Investig. Rep. 5233 (2010), 196.